

**ATiO<sub>3</sub>/TiO (A=Pb, Sn) superlattice: bridging ferroelectricity and conductivity**

S. Raza,<sup>1,2</sup> R. Zhang,<sup>3</sup> N. Zhang,<sup>4</sup> Z. Li,<sup>5</sup> L. Liu,<sup>6</sup> F. Zhang,<sup>1</sup> D. Wang,<sup>1, a)</sup> and C.-L. Jia<sup>1,7</sup>

<sup>1</sup>*School of Microelectronics & State Key Laboratory for Mechanical Behavior of Materials, Xi'an Jiaotong University, Xi'an 710049, China*

<sup>2</sup>*School of Energy and Environment, City University of Hong Kong, Kowloon 999077, Hong Kong Special Administrative Region, China*

<sup>3</sup>*School of Engineering and Materials Science, Queen Mary University of London, London E1 4NS, United Kingdom*

<sup>4</sup>*Electronic Materials Research Laboratory–Key Laboratory of the Ministry of Education and International Center for Dielectric Research, Xi'an Jiaotong University, Xi'an 710049, China*

<sup>5</sup>*School of Materials Science and Engineering, University of Science and Technology Beijing, Beijing 100083, China*

<sup>6</sup>*College of Materials Science and Engineering, Guilin University of Technology, Guilin 541004, China*

<sup>7</sup>*Ernst Ruska Center for Microscopy and Spectroscopy with Electrons, Forschungszentrum, Jülich 52425, Germany*

(Dated: February 11, 2020)

We propose to insert TiO layers to perovskite ATiO<sub>3</sub> to form a superlattice and use first-principles calculations to investigate its basic properties. Our computational analysis shows that the structure, which consists of repeated ATiO<sub>3</sub> and TiO layers, has strong anisotropic conductivity. The structure immediately suggests a possible control of its conductivity by ion displacements related to its intrinsic ferroelectricity. In addition, we have obtained the structural information of its low-energy phases with the aid of phonon calculation and examined their evolution with epitaxial strain. Since the number of possible combinations is huge, we have therefore suggested an approach to mix perovskites and simpler metal-oxides to build materials with novel properties.

---

<sup>a)</sup>Electronic mail: [dawei.wang@xjtu.edu.cn](mailto:dawei.wang@xjtu.edu.cn)

## I. INTRODUCTION

The crystal structure of a material is one of the most important factors that determines its properties. For ferroelectric and piezoelectric materials, strain engineering has been used to enhance their performances<sup>1-7</sup> by tuning the in-plane lattice constant and ion displacements, and its influence on structural properties and polarization has been extensively studied. In addition to applying strain, combing ferroelectricity with other functionality (e.g., conductivity) in a single structure can potentially induce their mutual control, crucial for technological applications. The most important example is probably the LaAlO<sub>3</sub>/SrTiO<sub>3</sub> heterointerface, where the polarity discontinuity creates high-mobility electron gas<sup>8</sup> that enables the conductivity, which is rather surprising since both materials are insulators. Later, Lee *et al* replaced the polar LaAlO<sub>3</sub> with a polarizable gel, resulting in continuously tunable electron density on the interface<sup>9</sup>.

Researchers have proposed other superstructures to go beyond perovskite (ABO<sub>3</sub>) by combining it with other oxides. One well known combination is a perovskite interfacing with its constituent oxide where an extra rocksalt AO layer is added (with some in-plane shift) to  $n$  layers of ABO<sub>3</sub> ( $n = 1, 2, 3 \dots$ ), resulting in the  $A_{n+1}B_nO_{3n+1}$  structure<sup>10,11</sup> [see Fig. S1 (a) in the supplemental material<sup>12</sup>], referred to as the Ruddlesden-Popper (RP) phase, which has been experimentally realized<sup>13,14</sup> and its ferroelectric nature investigated for, e.g., Sn<sub>2</sub>TiO<sub>4</sub> and Pb<sub>2</sub>TiO<sub>4</sub><sup>10,15</sup>. In addition, Aurivillius-type layered structure has also been investigated<sup>16-18</sup> and recently proposed for energy storage<sup>19</sup>.

One may wonder if tunable conductivity can be achieved by mixing perovskite with simpler metal-oxides. Such a possibility indeed exists by inserting extra BO layers into a perovskite (which means TiO for ATiO<sub>3</sub>). While the misfit strain between ATiO<sub>3</sub> and TiO can be huge, given the recent discovery of giant polarization in highly strained ( $\sim 16.5\%$  tensile strain) crystal structure<sup>6</sup>, the ATiO<sub>3</sub>/TiO superlattice is plausible and worth first-principles investigation to establish its basic properties. Furthermore, while perovskites junctioned with TiO<sub>2</sub> have been explored to optimize their photoelectrochemical, photocatalytic, and dielectric properties<sup>20,21</sup>, the use of TiO lacks any prior investigation.

In this work, we investigate superlattices made of ATiO<sub>3</sub>/TiO ( $A = \text{Pb, Sn}$ ) with and without epitaxial strain. The superlattice is built by stacking the (001) planes of simple metal-oxides, resulting in the AO-TiO<sub>2</sub>-2TiO-TiO<sub>2</sub> structure, which has 12 atoms in each unit cell shown as the dotted-line-enclosed region in Fig. 1 (a), noting that the TiO layer has two Ti atoms and two O atoms in

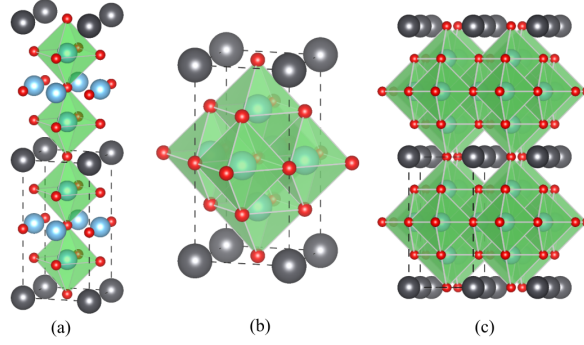


Figure 1. (a) The  $1 \times 1 \times 2$  superlattice model of the proposed  $\text{ATiO}_3/\text{TiO}$  structure, which is grown along the  $z$ -direction. (b-c) The  $1 \times 1 \times 1$  and  $2 \times 2 \times 2$  superlattice model viewed at different angles to emphasize the oxygen octahedron inside. The dark grey, blue, and red spheres represent A (Pb or Sn), Ti, and O atoms, respectively.

one unit cell. The general formula for such a superlattice is  $(\text{ATiO}_3)_n(2\text{TiO})_m(\text{TiO}_2)$  ( $n = 1, 2, 3 \dots$ ,  $m = 1, 3, 5 \dots$ ), different from the RP structure  $(\text{A}_{n+1}\text{Ti}_n\text{O}_{3n+1})$  as shown in Fig. S1<sup>12</sup>. The TiO layer has been properly shifted in the  $x$ - $y$  plane to allow the oxygen atoms to sit above the Ti atom of  $\text{ATiO}_3$ , maintaining the  $\text{TiO}_6$  octahedra that strengthens the bonding of the TiO and  $\text{TiO}_2$  layers, where edge-sharing oxygen octahedra can be seen in Fig. 1 (b) and (c). The specific arrangement of oxygen octahedra likely deactivates their tilting. In addition to the structural novelty of the superlattice, TiO is known to be stable and metallic<sup>22–24</sup> and nano TiO crystal is a type-II superconductor<sup>25</sup> while  $\text{ATiO}_3$  ( $A = \text{Pb}, \text{Sn}$ ) is an insulator with strong ferroelectricity. Therefore, the proposed superlattice is an ordered structure formed by repeating different functional units, following the recently proposed research paradigm<sup>26</sup>. In this paper, we will investigate their structural and electronic properties using first-principles calculations. As we will show, such a structure bridges ferroelectricity and conductivity that is potentially tunable by the relative number of the TiO and the  $\text{ATiO}_3$  layers.

## II. METHOD

In first-principles calculations, the atomic positions and lattice constants are relaxed until both the force on an ion and the stress fall below  $0.005 \text{ eV}/\text{\AA}$  using the projector augmented plane wave (PAW) method as implemented in the GPAW software package<sup>27</sup>. The localized density approximation (LDA) is used with a cut-off energy of  $750 \text{ eV}$  to ensure the convergence. A  $4 \times$

$4 \times 2$  Monkhorst-Pack<sup>28</sup> sampling is used for the  $k$ -space integration. The used valence orbitals are: Sn ( $5s\ 5p\ 4d$ ), Pb ( $6s\ 6p\ 5d$ ), Ti ( $3s\ 3p\ 4s\ 3d$ ) and O ( $2s\ 2p$ ). All the crystal structures are created using Atomic Simulation Environment (ASE)<sup>29</sup> and visualized with VESTA<sup>30</sup>. With such a setup, we first obtained the tetragonal structures of SnTiO<sub>3</sub> and PbTiO<sub>3</sub>, which are compared to literature<sup>31</sup>, showing excellent agreements (see Tab. S1<sup>12</sup>). The initial lattice constants of SnTiO<sub>3</sub> and PbTiO<sub>3</sub> with ions in their ideal positions ( $P4/mmm$  symmetry) have the lattice parameters of  $a = 3.79$ ,  $c = 4.175\ \text{\AA}$ <sup>32</sup>, and  $a = 3.89$ ,  $c = 4.15\ \text{\AA}$ <sup>6</sup>, respectively, whereas the rocksalt TiO has a lattice constant of  $a = 4.17\ \text{\AA}$ <sup>33</sup> with the  $Fm\bar{3}m$  symmetry, indicating a stretching of the perovskite part in the  $x$ - $y$  plane when its lattice is coherently kept with TiO. We note, under external epitaxial strain, the lattice mismatch between ATiO<sub>3</sub> and TiO can be adjusted.

### III. RESULTS AND DISCUSSION

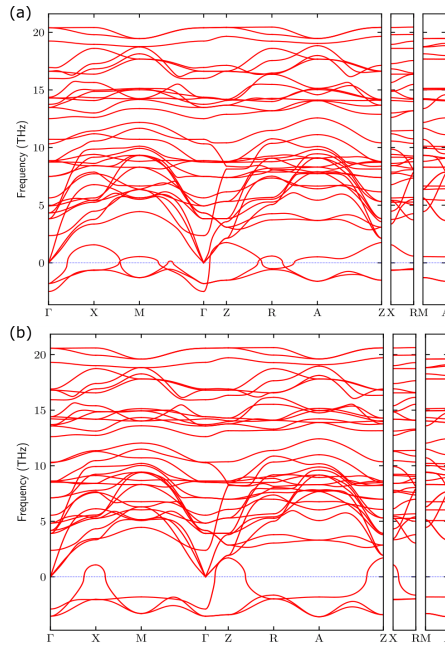


Figure 2. Phonon band structure for PbTiO<sub>3</sub>/TiO (a) and SnTiO<sub>3</sub>/TiO (b).

We use Phonopy<sup>34</sup> to perform phonon calculation on the original superlattice ( $P4/mmm$  symmetry<sup>35</sup>) in order to obtain unstable phonon modes and construct low-energy structural phases accordingly. To this end, the lattice constants of the structure are optimized but ions are fixed on their initial (ideal) positions. We have used a  $2 \times 2 \times 2$  supercell (96 atoms) to get accurate results on the high-symmetry points (e.g.,  $\Gamma$ ,  $X$ ,  $R$ , and  $M$  points in the Brillouin-zone). Figure 2 shows

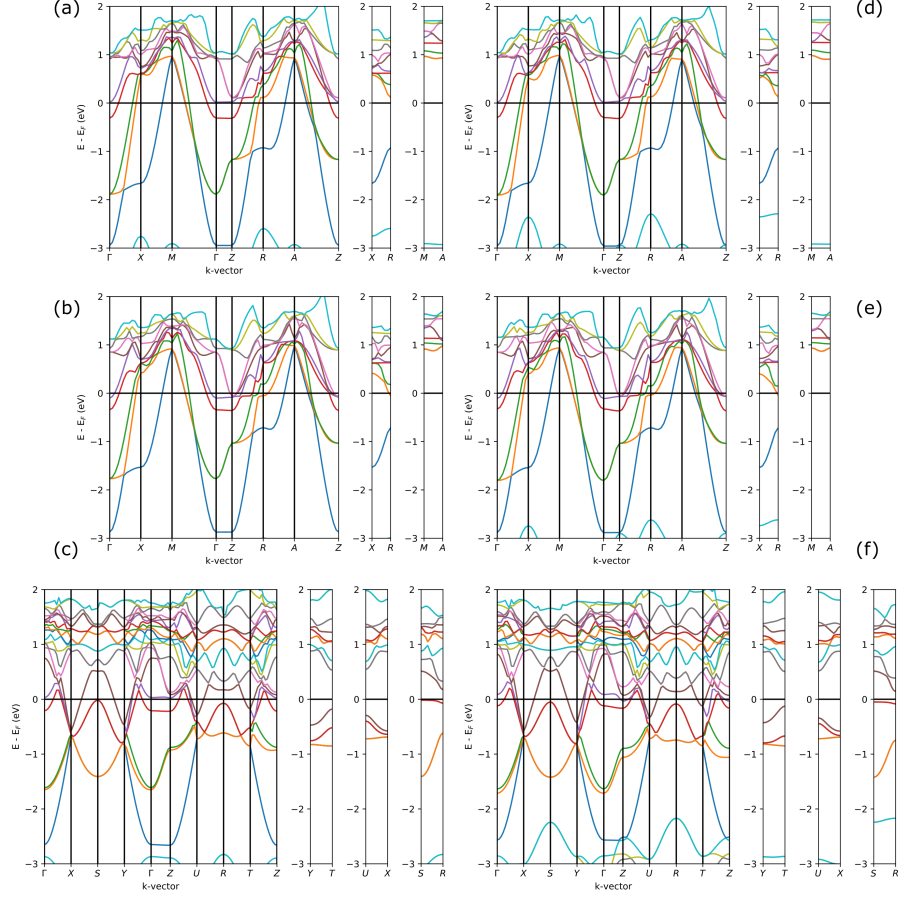


Figure 3. Bandstructure of  $\text{PbTiO}_3/\text{TiO}$  (left panel) and  $\text{SnTiO}_3/\text{TiO}$  (right panel) in its  $P4/mmm$  phase. (a) Ions in ideal positions, cell optimized; (b) Ions and cells are both relaxed; (c) The  $Amm2$  phase (using the basis of  $\mathbf{a} + \mathbf{b}$  and  $\mathbf{a} - \mathbf{b}$ , therefore the directions in the reciprocal space is different from (a) and (b)). (d-f) Counterparts of (a-c) for  $\text{SnTiO}_3/\text{TiO}$  with (f) having the  $Cm$  phase.

that the phonon dispersion has the strongest instability at the  $\Gamma$  point [ $\mathbf{k} = (0,0,0)$ ], providing clues to the most likely structural phases. We note the  $\Gamma$  point instability is inherent to many ferroelectric perovskites including  $\text{PbTiO}_3$  and  $\text{SnTiO}_3$ .

Based on the phonon spectrum and common ferroelectric phases of perovskites, we obtained several structural phases of the  $\text{ATiO}_3/\text{TiO}$  superlattice by displacing Ti in the perovskite layer along the high-symmetry directions, forming the  $P4/mmm, P4mm, Pm, Amm2, Pmm2$ , and  $Cm$  phases<sup>36</sup>. The overall symmetry of the superlattice is checked both before and after their structural relaxation. Table I displays the information of the relaxed  $\text{SnTiO}_3/\text{TiO}$  and  $\text{PbTiO}_3/\text{TiO}$ , which have the  $Cm$  and  $Amm2$  phase as the ground state, respectively. The perovskite part of the relaxed  $\text{ATiO}_3/\text{TiO}$  experiences a tensile strain of about 3-5% while the TiO part undergoes a compress-

Space group	$a(\text{\AA})$	$b(\text{\AA})$	$c(\text{\AA})$	$\alpha$	$\beta$	$\gamma$	Energy	
SnTiO <sub>3</sub> /TiO	$P4/mmm$	4.0067	4.0067	7.8791	90	90	90	172.6
	$P4mm$	4.0069	4.0069	7.9261	90	90	90	156.4
	$Pmm2$	4.0116	4.0117	7.9178	90	90	90	22.9
	$Amm2$	4.015	4.015	7.9039	90	90	89.33	22.4
	$Pm$	4.011	4.012	7.9193	90	89.98	90	22.8
	$Cm$	4.013	4.013	7.9125	89.98	89.98	89.54	0
PbTiO <sub>3</sub> /TiO	$P4/mmm$	4.012	4.012	7.8964	90	90	90	37.4
	$P4mm$	4.013	4.013	7.8974	90	90	90	37.3
	$Pmm2$	4.023	4.000	7.8946	90	90	90	5.6
	$Amm2$	4.012	4.012	7.8950	90	90	89.88	0
	$Pm$	4.023	4.000	7.8957	90	89.99	90	5.4
	$Cm$	4.012	4.012	7.8946	89.98	89.98	89.87	0.1

Table I. Structural information of the ATiO<sub>3</sub>-TiO (A=Sn,Pb) superlattice after relaxation. Note the rocksalt TiO has a lattice constant of 4.177 Å and the energy unit is meV per formula.

sion of about 4%. The tensile strain forces the ATiO<sub>3</sub> component into a pseudocubic structure ( $a = b \simeq c/2$ ). The in-plane lattice constants of SnTiO<sub>3</sub>/TiO and PbTiO<sub>3</sub>/TiO are rather close since the rigid TiO layer is unable to compress further. Except the  $P4mm$  and  $P4/mmm$  phases, the structural phases have close energies, indicating that the ion displacement inside the  $x$ - $y$  plane is preferred. In addition, the SnTiO<sub>3</sub>/TiO has a stronger tendency to stay in the  $Cm$  phase with a nonzero polarization along  $z$ , an inherent property to SnTiO<sub>3</sub><sup>37</sup>.

Table S2<sup>12</sup> provides the ion displacements (in fractional coordinates) for the  $Cm$  and  $Amm2$  phases, showing large displacements of ions in the  $x - y$  plane and relatively small shifts in the  $z$  direction. It also indicates that SnTiO<sub>3</sub>/TiO has larger ion displacements than PbTiO<sub>3</sub>/TiO. Due to its smaller ionic size, the Sn atom exhibits a much larger (10 times larger) displacement than the Pb atoms. To further confirm that the  $Cm$  ( $Amm2$ ) phase is the ground state, we have also constructed other configurations suggested by the  $\Gamma$  point phonon eigenvector, removed all the symmetry constraints, and relaxed the structure again; but no new structural phases with lower energy were found.

Let us now turn to the electronic properties of ATiO<sub>3</sub>/TiO. Since PbTiO<sub>3</sub> and SnTiO<sub>3</sub> are in-

ulators, it is important to know how the TiO layer alters the electronic band structures. For TiO, we have calculated its band structure, agreeing well with literature<sup>22-24</sup>, confirming that TiO is a conductor (see Fig. S2<sup>12</sup>). Figure 3 displays the electronic band structure of PbTiO<sub>3</sub>/TiO (left column) and SnTiO<sub>3</sub>/TiO (right column). Figure 3(a) shows that the electronic band structure of PbTiO<sub>3</sub>/TiO in its original  $P4/mmm$  phase, which clearly demonstrates that the superlattice is still a conductor, while the  $\Gamma$  to  $Z$  line (related to the superlattice growth direction) is slightly above the Fermi level. Figure 3(b) shows the band structure when the ions are also relaxed. This structure is still a conductor, but the  $\Gamma$  to  $Z$  line has dropped below the Fermi level. While such a change is small, it implies a strong influence on the conductivity along the growth direction. For the lowest energy state we have found (with the  $Amm2$  symmetry), Fig. 3(c) shows that the  $\Gamma$  to  $Z$  line again rises above the Fermi level, but remains very close to it.

The electronic band structure along the  $\Gamma$ - $Z$  line shown in Figs. 3(a-c) indicates that the conductivity along the superlattice-growth direction can be quite sensitive to ion displacements. This connection is potentially important given the fact that both PbTiO<sub>3</sub> and SnTiO<sub>3</sub> are ferroelectric, a feature arising from their ion displacements. Moreover, in all the three cases shown in Figs. 3(a-c), the  $\Gamma$  to  $Z$  line is special in its flatness, indicating a huge electron/hole effective mass along the superlattice-growth direction, resulting in strong anisotropic conductivity. Figures 3(d-f) show that SnTiO<sub>3</sub>/TiO has similar behaviors on the  $\Gamma$  to  $Z$  line with some minor variations comparing to PbTiO<sub>3</sub>. Similar behavior with the Ruddlesden-Popper double-layered perovskite La<sub>3</sub>Ni<sub>2</sub>O<sub>7</sub> has been reported in recent years<sup>38,39</sup>.

Finally, let us briefly discuss epitaxial strain effects on ATiO<sub>3</sub>/TiO. We replicate the biaxial epitaxial strain by fixing the in-plane lattice constant. The misfit strain is calculated with  $\epsilon = (a - a_0) / a_0$  where  $a_0$  is the optimized lattice constant of the superlattice without the in-plane constraint. The energies of the structural phases versus the epitaxial strain are shown in Fig. 4, where the  $P4mm$  and  $P4/mmm$  phases are omitted due to their much higher energy. Figure 4(a) shows that SnTiO<sub>3</sub>/TiO has the  $Cm$  phase as the ground state for a wide range of misfit strain until  $a = 4.10 \text{ \AA}$  ( $\simeq 2.15\%$  tensile strain) when the  $Amm2$  phase becomes most stable. Figure 4(b) shows a similar behavior for the PbTiO<sub>3</sub>/TiO where the  $Cm$  is most stable phase until  $a = 4.05 \text{ \AA}$  ( $\simeq 0.95\%$  tensile strain)<sup>40</sup>. Over the whole misfit strain range, the  $Pm$  [with polarization direction  $(u, 0, w)$ ] and  $Pmm2$  [ $(u, 0, 0)$ ] phases are close in energy to the  $Amm2$  [ $(u, u, 0)$ ] and the  $Cm$  [ $(u, u, w)$ ] phases while their ion displacements are in different directions. Figure S3 shows the  $(c/2)/a$  ratio for ATiO<sub>3</sub>/TiO, which is adopted to compare to the  $c/a$  of simple ATiO<sub>3</sub>, de-

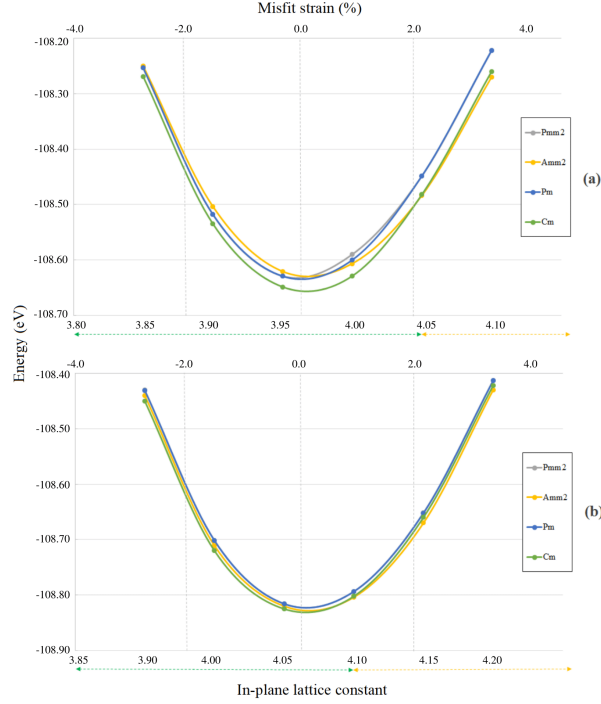


Figure 4. The energy versus the lattice constant for epitaxially strained SnTiO<sub>3</sub>/TiO (a) and PbTiO<sub>3</sub>/TiO (b) superlattice with the *Amm2*, *Pmm2*, *Pm*, and *Cm* symmetries..

creases with the in-plane lattice constant. The  $(c/2)/a$  of SnTiO<sub>3</sub>/TiO remains higher than that of PbTiO<sub>3</sub>/TiO since the tetragonality of the parent SnTiO<sub>3</sub> (1.13)<sup>41</sup> is larger than PbTiO<sub>3</sub> (1.065)<sup>42</sup>.

The proposed superlattice is composed of perovskite ATiO<sub>3</sub> and TiO layers. As a matter of fact, there are other layered metal-oxides in addition to the RP phase<sup>43</sup>. The Aurivillius phase was first proposed by Aurivillius with the general formula (Bi<sub>2</sub>O<sub>2</sub>)(A<sub>*n*-1</sub>B<sub>*n*</sub>O<sub>3*n*+1</sub>), where A and B are cations<sup>44</sup>. It can be thought of as alternating layers of Bi<sub>2</sub>O<sub>2</sub> and perovskites whose ferroelectric, magnetic, and dielectric properties have been extensively studied in the past<sup>16-18</sup>. The Dion-Jacobson series has the general formula A' (A<sub>*n*-1</sub>B<sub>*n*</sub>O<sub>3*n*+1</sub>), where A', A and B are cations<sup>45,46</sup>. This structure has an intermediate layer of A' atoms (often alkali metal) between perovskite blocks<sup>46</sup>. More recently, Tsujimoto *et al* managed to remove more oxygens from conventional perovskite SrFeO<sub>3-*x*</sub>, producing a structure with alternating layers of FeO<sub>2</sub> and Sr<sup>47</sup>. The superlattice we proposed here are different from these known layered structures.

There are many simple oxides and perovskites to choose from to build the proposed superlattice. For instance, possible monoxides with the rocksalt structures include MgO ( $a = 4.217 \text{ \AA}$ ), MnO ( $a = 4.446 \text{ \AA}$ ), NiO ( $a = 4.178 \text{ \AA}$ ), CoO ( $a = 4.263 \text{ \AA}$ ), and NbO ( $a = 4.2101 \text{ \AA}$ ). Among



them, NbO is metallic<sup>48,49</sup> and NiO and CoO are antiferromagnetic. Such combinations have the potential to generate novel materials with special properties. Since the growth of the RP phase has already used techniques like reactive/hybrid molecular beam epitaxy<sup>13,14</sup>, the growth of the proposed superlattice does not seem particularly difficult, also noting that TiO does not add any new element to  $\text{ATiO}_3$ . The  $\text{ATiO}_3/\text{TiO}$  superlattice can be fabricated by alternating growth of the  $\text{ATiO}_3$  and TiO layers using oxide molecular beam epitaxy (O-MBE)<sup>39</sup>, pulsed laser deposition (PLD), or atomic layer deposition (ALD) methods. Monitoring with the *in situ* reflected high energy electron diffraction (RHEED), the thickness of both the  $\text{ABO}_3$  and the TiO layers, as well as their periodicity, can be precisely controlled. The epitaxial strain can be induced by properly selecting single crystal perovskite substrates. For instance, the  $\text{BaTiO}_3$  (001) and  $(1-x)\text{PbMg}_{1/3}\text{Nb}_{2/3}\text{O}_3-x\text{PbTiO}_3$  substrates can induce tensile strain while the  $\text{SrTiO}_3$  (001),  $\text{LaAlO}_3$  (001) substrates can induce compressive strain.

#### IV. CONCLUSION

In summary, we have proposed a superlattice with TiO layers inserted into the perovskite  $\text{PbTiO}_3$  or  $\text{SnTiO}_3$ , investigated their structural and electronic properties, finding that they are anisotropic conductors with tunable conductivity that is sensitive to ion displacements. Such a feature can couple conductivity to ferroelectricity, enabling the control of conductivity with electric field or strain. Furthermore, the proposed structure is automatically a micro-multilayer ceramic capacitor and can have large permittivity due to the Maxwell-Wagner effect. We finally note that, in growing such superlattice, there is no constraint on the ratio between the number of  $\text{ATiO}_3$  layers and the TiO layers, which can be used to tune special properties of the resulting superlattices.

#### ACKNOWLEDGMENTS

This work is financially supported by the National Natural Science Foundation of China, Grant No. 11974268, 11574246, and U1537210. D.W. also thanks support from the Chinese Scholarship Council (201706285020).

## REFERENCES

- <sup>1</sup>R. von Helmolt, J. Wecker, B. Holzapfel, L. Schultz, and K. Samwer, *Phys. Rev. Lett.* **71**, 2331 (1993).
- <sup>2</sup>J.-P. Locquet, J. Perret, J. Fompeyrine, E. Mächler, J. W. Seo, and G. Van Tendeloo, *Nature* **394**, 453 (1998).
- <sup>3</sup>M. Lee, T. Nath, and C. Eom, *Appl. Phys. Lett.* **77**, 3547, (2000).
- <sup>4</sup>H. Béa, B. Dupé, S. Fusil, R. Mattana, E. Jacquet, B. Warot-Fonrose, F. Wilhelm, A. Rogalev, S. Petit, V. Cros, A. Anane, F. Petroff, K. Bouzehouane, G. Geneste, B. Dkhil, S. Lisenkov, I. Ponomareva, L. Bellaiche, M. Bibes, and A. Barthélémy, *Phys. Rev. Lett.* **102**, 217603 (2009).
- <sup>5</sup>D. G. Schlom, L.-Q. Chen, C. J. Fennie, V. Gopalan, D. A. Muller, X. Pan, R. Ramesh, and R. Uecker, *MRS Bull.* **39**, 118 (2014).
- <sup>6</sup>L. Zhang, J. Chen, L. Fan, O. Dieguez, J. Cao, Z. Pan, Y. Wang, J. Wang, M. Kim, S. Deng, J. Wang, H. Wang, J. Deng, R. Yu, J.F. Scott, and X. Xing, *Science* **361**, 494 (2018).
- <sup>7</sup>T. Nakashima, D. Ichinose, Y. Ehara, T. Shimizu, T. Kobayashi, T. Yamada, and H. Funakubo, *Appl. Phys. Lett.* **110**, 122902 (2017).
- <sup>8</sup>A. Ohmoto and H. Y. Hwang, *Nature* **427**, 423 (2004).
- <sup>9</sup>M. Lee, J. R. Williams, S. Zhang, C. Frisbie, and D. Goldhaber-Gordon, *Phys. Rev. Lett.* **107**, 256601 (2011).
- <sup>10</sup>C. Fennie and K. Rabe, *Phys. Rev. B* **71**, 100102(R) (2005).
- <sup>11</sup>S. Ruddlesden and P. Popper, *Acta Crystallogr.* **11**, 54 (1958).
- <sup>12</sup>The supplemental material is submitted along with the manuscript.
- <sup>13</sup>J. H. Haeni, C. D. Theis, and D. G. Schlom, *Appl. Phys. Lett.* **78**, 3292 (2001).
- <sup>14</sup>R. C. Haislmaier, G. Stone, N. Alem, and R. E. Herbert, *Appl. Phys. Lett.* **109**, 043102 (2016).
- <sup>15</sup>R. Zhang, D. Wang, X. Zhu, X. Wei, and Z. Xu, *J. Appl. Phys.* **116**, 174101 (2014).
- <sup>16</sup>J.-B. Li, Y. P. Huang, G. H. Rao, G. Y. Liu, J. Luo, J. R. Chen, and J. K. Liang, *Appl. Phys. Lett.* **96**, 222903 (2010).
- <sup>17</sup>J. Yang, L. H. Yin, Z. Liu, X. B. Zhu, W. H. Song, J. M. Dai, Z. R. Yang, and Y. P. Sun, *Appl. Phys. Lett.* **101**, 012402 (2012).
- <sup>18</sup>B. Yuan, J. Yang, J. Chen, X. Z. Zuo, L. H. Yin, X. W. Tang, X. B. Zhu, J. M. Dai, W. H. Song, and Y. P. Sun, *Appl. Phys. Lett.* **104**, 062413 (2014).
- <sup>19</sup>Z. Tang, J. Chen, B. Yang, and S. Zhao, *Appl. Phys. Lett.* **114**, 163901 (2019).

- <sup>20</sup>J. S. Jang, C.W. Ahn, S.S. Won, J.H. Kim, W. Choi, B. Lee, J. Yoon, H.G. Kim, and J.S. Lee, J. Phys. Chem. C **121**, 15063 (2017).
- <sup>21</sup>Y. Zeng, A. A. Bokov, D. Wang, F. Xiang, H. Wang, Ceram. Int. **44**, 17548 (2018).
- <sup>22</sup>S. P. Denker, J. Appl. Phys. **37**, 142 (1966).
- <sup>23</sup>R. Ahuja, O. Eriksson, J. M. Wills, and B. Johansson, Phys. Rev. B **53**, 3072 (1996).
- <sup>24</sup>Y. O. Ciftci, Y. Unlu, K. Colakoglu, and E. Deligoz, Phys. Scr. **80**, 025601 (2009).
- <sup>25</sup>J. Xu, D. Wang, H. Yao, K. Bu, J. Pan, J. He, F. Xu, Z. Hong, X. Chen, and F. Huang, Adv. Mater. **30**, 1706240 (2018).
- <sup>26</sup>K. Chen and L. Li, Adv. Mater **31**, 1901115 (2019).
- <sup>27</sup>J. Enkovaara, C. Rostgaard, J.J. Mortensen, J. Chen, M. Duřak, L. Ferrighi, J. Gavnholt, C. Glinsvad, V. Haikola, H.A. Hansen, H.H. Kristoffersen, M. Kuisma, A.H. Larsen, L. Lehtovaara, M. Ljungberg, O. Lopez-Acevedo, P.G. Moses, J. Ojanen, T. Olsen, V. Petzold, N.A. Romero, J. Stausholm-Møller, M. Strange, G.A. Tritsarlis, M. Vanin, M. Walter, B. Hammer, H. Häkkinen, G.K.H. Madsen, R.M. Nieminen, J.K. Nørskov, M. Puska, T.T. Rantala, J. Schiøtz, K.S. Thygesen and K.W. Jacobsen, J. Phys.: Condens. Matter **22**, 253202 (2010).
- <sup>28</sup>H. J. Monkhorst and J. D. Pack, Phys. Rev. B **13**, 5188 (1976).
- <sup>29</sup>Atomic Simulation Environment (ASE), <https://wiki.fysik.dtu.dk/ase>.
- <sup>30</sup>K. Momma and F. Izumi, J. Appl. Cryst. **44**, 1272 (2011).
- <sup>31</sup>Y. Xue, D. Chen, Y. Wang, Y. Tang, Y. Zhu, and X. Ma, Philos. Mag **95**, 2067 (2015).
- <sup>32</sup>S. Matar, I. Baraille, and M. Subramanian, Chem. Phys. **355**, 43 (2009).
- <sup>33</sup>D. Wang, C. Huang, J. He, X. Che, H. Zhang, F. Huang, ACS Omega **2**, 1036 (2017).
- <sup>34</sup><https://atztogo.github.io/phonopy/>
- <sup>35</sup>We note that alternately stacking  $\text{ATiO}_3$  layer with TiO layer is equivalent to replacing every second AO layer with the TiO layer, resulting in the  $P4/mmm$  symmetry if the original cubic perovskite cells are not distorted.
- <sup>36</sup>O. Dieguez and D. Vanderbilt, Phase Trans. **81**, 607 (2008).
- <sup>37</sup>D. Wang, L. Liu, J. Liu, N. Zhang, and X. Wei, Chin. Phys. B **27**, 127702 (2018).
- <sup>38</sup>J. Lee, G. Luo, I. Tung, S. Chang, Z. Luo, M. Malshe, M. Gadre, A. Bhattacharya, S. Nakhmanson, J. A. Eastman, H. Hong, J. Jellinek, D. Morgan, D. D. Fong and J. W. Freeland, Nat. Mater. **13**, 879 (2014).
- <sup>39</sup>Y Mochizuki, H. Akamatsu, Y. Kumagai, and Fumiyasu Oba, Phys. Rev. Mater. **2**, 125001 (2018).

- <sup>40</sup>For epitaxially strained PbTiO<sub>3</sub>/TiO, the results here indicate that the *Cm* phase can be slightly lower in energy (~0.16 meV) than the *Amm2* phase, different from the result shown in Tab. **I**. This is because the angle between the in-plane *x* and *y* axis ( $\gamma$ ) is not allowed to change when epitaxially strained, making it different from the free relaxation shown in Tab. **I**.
- <sup>41</sup>W. Parker, J. Rondinelli, and S. Nakhmanson, Phys. Rev. B **84**, 245126 (2011).
- <sup>42</sup>G. Saghi-Szabo, R. Cohen, and H. Krakauer, Phys. Rev. Lett. **80**, 4321 (1998).
- <sup>43</sup><https://www.princeton.edu/~cavalab/tutorials/public/structures/perovskites.html>
- <sup>44</sup>K. Kendall, C. Navas, J. Thomas, and H.-C. zur Loye, Chem. Mater. **8**, 642 (1996).
- <sup>45</sup>J. Choy, J. Kim, S. Kim, and J. Sohn, Chemistry of Materials **13**, 906 (2001).
- <sup>46</sup>C. Fennie and K. Rabe, Appl. Phys. Lett. **88**, 262902 (2006).
- <sup>47</sup>Y. Tsujimoto, C. Tassel, N. Hayashi, T. Watanabe, H. Kageyama, K. Yoshimura, M. Takano, M. Ceretti, C. Ritter & W. Paulus, Nature **450**, 1062 (2007).
- <sup>48</sup>R. Tao, R. Todorovic, J. Liu, R. J. Meyer, A. Arnold, W. Walkosz, P. Zapol, A. Romanenko, L. D. Cooley, and R. F. Klie, J. Appl. Phys. **110**, 124313 (2011).
- <sup>49</sup>A. Dhamdhere, T. Hadamek, A. Posadas, A. Demkov, and D.J. Smith, J. Appl. Phys. **120**, 245302 (2016).